

## Choice of suitable micellar catalyst for 2,2'-bipyridine-promoted chromic acid oxidation of glycerol to glyceraldehyde in aqueous media at room temperature

Aniruddha Ghosh · Rumpa Saha ·  
Kakali Mukherjee · Sumanta K. Ghosh · Pintu Sar ·  
Susanta Malik · Bidyut Saha

Received: 16 August 2012 / Accepted: 19 September 2013  
© Springer Science+Business Media Dordrecht 2013

**Abstract** The micellar catalyzed 2,2'-bipyridine (bipy)-promoted oxidation of glycerol to glyceraldehyde by chromic acid is investigated under the criteria  $[\text{glycerol}]_{\text{T}} \gg [\text{Cr(VI)}]_{\text{T}}$  at 30 °C. The critical micellar concentrations values of the three representative surfactants, *N*-cetylpyridinium chloride (CPC), sodium dodecyl sulphate (SDS), and TX-100, are determined by conductometric and spectrophotometric methods. The oxidized product glyceraldehyde is identified by 2,4-DNP test and FTIR spectral measurement. The pseudo-first-order rate constants ( $k_{\text{obs}}, \text{s}^{-1}$ ) are calculated from the slope of plots of  $\ln(A_{450})$  versus time ( $t$ ) which are linear. From these plots, the kinetic parameter  $k_{\text{eff}}$  values are calculated and the  $k_{\text{eff}}$  value of SDS-catalyzed bipy-promoted reaction path was found to be highest among all the combinations. In the bipy-promoted oxidation path, Cr(VI)–bipy complex is the main active oxidant which undergoes attack by the substrate to form the product. The active oxidant Cr(VI)–bipy complex reacts with glycerol to form a ternary complex which undergoes redox decomposition in a rate-limiting step. Here, the anionic surfactant SDS and the neutral surfactant TX-100 both catalyze the reaction in the presence of bipy, whereas the cationic surfactant CPC and neutral surfactant TX-100 inhibit the reaction in the absence of bipy. SDS is found to be the most suitable micellar catalyst for the bipy-promoted chromic acid oxidation of glycerol.

**Keywords** 2,2'-Bipyridine (bipy) · Glycerol ·  $[\text{Cr(VI)}]_{\text{T}}$  · CMC · CPC · SDS · TX-100

---

A. Ghosh · R. Saha · K. Mukherjee · S. K. Ghosh · P. Sar · S. Malik · B. Saha (✉)  
Homogeneous Catalysis Laboratory, Department of Chemistry, The University of Burdwan,  
Golapbag, Burdwan 713104, WB, India  
e-mail: b\_saha31@rediffmail.com

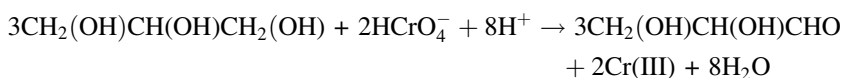
R. Saha  
Bishnupur K.G. Engineering Institute, Bankura, WB, India

## Introduction

Chromium(VI)-based oxidizing agents have been used to develop a good number of reagents, some of which have become quite popular and perform well as oxidizing agents [1]. Some of the important entries in the list of the reagents are pyridinium chlorochromate, pyridinium dichromate, pyridinium fluorochromate, pyridinium bromochromate, quinolinium fluorochromate, and prolinium chlorochromate. The syntheses involving these oxidants have been carried out mostly in less polar solvents, such as dichloromethane and trichloromethane, though the majority of kinetic measurements have been made only in polar solvents like aqueous acetic acid [2]. Problems in the use of chromium(VI) complexes as oxidation reagents include the lack of selectivity in oxidations, safety hazards associated with the use of large quantities of toxic compounds, cumbersome preparation, and potential danger (ignition) in handling, difficulties in terms of product, waste disposal, and the need for aqueous acidic or basic conditions for reactions of chromate salts [3]. Hexavalent chromium compounds are widely used as oxidizing agents mainly for carbonyls and alcohols in aqueous and non-aqueous media [4, 5]. A non-aqueous medium is introduced for one-step oxidation. Chromium chemistry is mainly dominated by two oxidation states, +3 and +6. In addition to non-toxic trivalent chromium, an amount of hexavalent chromium remains in the industrial effluents. There are two problems. Hexavalent chromium is carcinogenic [6–8] and a non-aqueous medium is not environmentally friendly [9, 10]. Use of large excesses of substrate over hexavalent chromium and aqueous medium can solve the problem. Academia and industry have been focused on the use of biorenewables for the production of chemicals and clean fuels. One biorenewable feedstock is glycerol, which can be found naturally in the form of fatty acid esters and also as important intermediates in the metabolism of living organisms. Glycerol is a highly functionalized compound and, in particular, its oxidation leads to a complex reaction network, in which a large number of products can be formed. Therefore, control of selectivity to the desired product would be highly advantageous [11]. The choice of  $K_2Cr_2O_7$  in aqueous micellar media is due to the control and selective oxidation of glycerol to glyceraldehyde by maintaining pseudo-first-order criteria. Glyceraldehyde is an important ingredient in the organic synthesis of glyceraldehyde-3-phosphate dehydrogenase which is a well-studied glycolytic protein with energy production as its implied occupation [12]. Glyceraldehyde is an example of a small chiral building block of great interest because of the wide applicability of its structural motif [13]. Water is one of the universal green solvents compared to other hazardous organic solvents, therefore the oxidation of glycerol has been carried out in aqueous media. This will produce one-step oxidation and total conversion of hexavalent chromium to trivalent chromium. Micellar solutions have versatile uses in the fields of chemistry, biochemistry, pharmacy, medicine, and industry. Different kinds of reactions, such as hydrolytic, oxidation, reduction, and photochemical, are significantly influenced by micelles [14–16]. The property of micelle formation in solution gives surfactants excellent solubilization properties [17]. A fundamental property of surfactants is their ability to form micelles in solution. This property is due to the presence of both hydrophobic and hydrophilic

groups in each surfactant molecule. As the title reaction is very slow, suitable combinations of micellar catalyst [18–22] and promoter [23–28] are used to speed up the reaction. In this work, we have studied the efficiency of the suitable combination of 2,2'-bipyridine (bipy) and micellar catalyst for the chromic acid oxidation of glycerol to glyceraldehyde. The micellar catalyzed picolinic acid and phenanthroline-promoted glycerol oxidation by chromic acid has been previously studied [27]. During the oxidation, three different types of surfactants: *N*-cetylpyridinium chloride (CPC) as cationic, sodium dodecyl sulphate (SDS) as anionic, and Triton X-100- as neutral non-functional micellar catalyst, have been used.

The chromic acid oxidation of glycerol is represented as follows:



## Experimental

### Instrumentation

Solutions of the oxidant and reaction mixtures containing known quantities of the substrate (i.e. glycerol), and promoter (bipy) were prepared under the kinetic conditions  $[\text{glycerol}]_{\text{T}} \gg [\text{Cr(VI)}]_{\text{T}}$ . Acid and other necessary chemicals were separately thermostated ( $\pm 0.10$  °C). The reaction was initiated by mixing requisite amounts of the oxidant with the reaction mixture. Progress of the reaction was monitored by following the decay of Cr(VI) at 450 nm wave length at different time intervals with a UV–Vis (UV–Vis–NIR-3600; Shimadzu) spectrophotometer. Quartz cuvettes of path length 1 cm were used. The pseudo-first-order rate constants ( $k_{\text{obs}}$ ,  $\text{s}^{-1}$ ) were calculated from the slope of plots of  $\ln(A_{450})$  versus time ( $t$ ) (Fig. 1), which were linear [5]. A large excess ( $\geq 15$ -fold) of reductant was used in all kinetic runs. No interference was observed due to other species at 450 nm. The scanned spectra, the spectrum after completion of the reaction and other spectra, were recorded with a UV–Vis spectrophotometer (UV-1800; Shimadzu). Rate constants of fast reactions are determined with the help of astopped flow spectrophotometer (SX20 Spectrometer).

Determination of critical micellar concentration (CMC) of CPC, SDS and TX-100

The CMC values of CPC and SDS were measured by the conductometric method. The conductivity of the different concentrated solutions of CPC and SDS was measured with a conductivity cell (CON 6000, cell constant  $1 \text{ cm}^{-1}$ ) provided with a built-in temperature sensor immersed in the beaker containing the surfactant solutions. The temperature was set to 30 °C (Table 1). All the conductivity measurements were recorded with the help of a water analyzer kit (Eutech instruments, CyberScan PCD 6500 Series Meters). Typical experimental

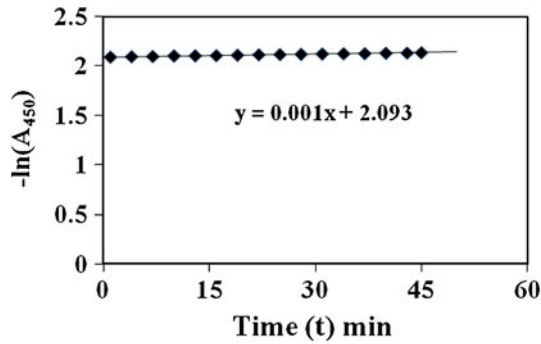
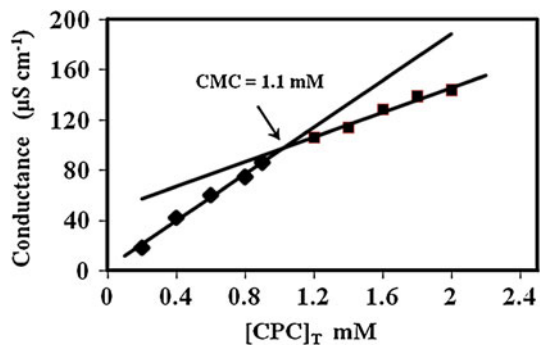


**Fig. 1** Representative first-order plot to evaluate the pseudo-first-order rate constant ( $k_{\text{obs}}$ ) for Cr(VI) oxidation of glycerol in an unpromoted path in aqueous medium.  $[\text{glycerol}]_{\text{T}} = 75 \times 10^{-4} \text{ mol dm}^{-3}$ ,  $[\text{Cr(VI)}]_{\text{T}} = 5 \times 10^{-4} \text{ mol dm}^{-3}$ ,  $[\text{H}_2\text{SO}_4]_{\text{T}} = 0.5 \text{ mol dm}^{-3}$ , Temp = 30 °C

**Table 1** CMC values at 30 °C temperature

Surfactant	Name of surfactant	Method	CMC (mM)
Cationic	CPC	Conductometric	8.2
Anionic	SDS	Conductometric	1.1
Neutral	TX-100	Spectrophotometric	0.24

**Fig. 2** Conductance against  $[\text{CPC}]_{\text{T}}$  plot; the intersection point is CMC of CPC at 1.1 mM. Temp = 30 °C



observations are presented in Figs. 2 and 3. The breaks obtained in the region of the CMC for solutions containing these two surfactants separately. From the plot of conductance versus concentration of CPC and SDS (Figs. 2, 3), the CMC of SDS and CPC were found at 1.1 and 8.2 mM, respectively, at 30 °C. These CMC values agree nicely with the established values established earlier [29, 30].

The CMC of TX-100 was analyzed by interaction with a saturated aqueous solution of iodine with varying concentration (below and above CMC) of TX-100 solution. The CMC value of TX-100 was determined by recording the absorbance values of the solutions containing the mixture of TX-100 and  $\text{I}_2$  solution after

**Fig. 3** Conductance against  $[\text{SDS}]_T$  plot; the intersection point is CMC of SDS at 8.2 mM. Temp = 30 °C

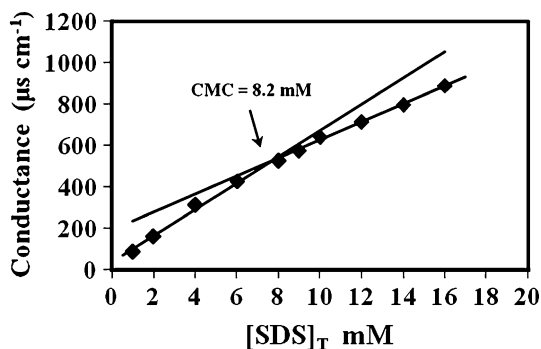
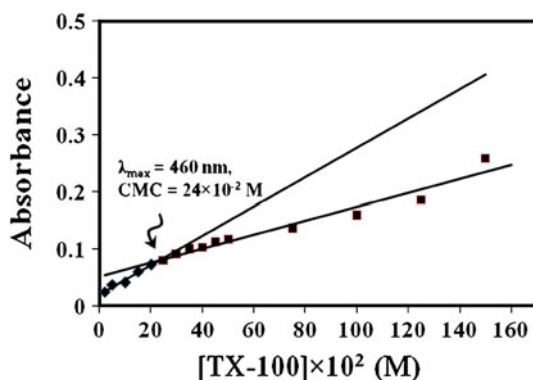


**Fig. 4** Plot of absorbance versus concentration of TX-100 with iodine solution at 460 nm. The break point is the CMC of TX-100. Temp = 30 °C



temperature equilibration at 30 °C at 460 nm with a UV–Vis spectrophotometer (UV-1800; Shimadzu). The CMC values obtained for TX-100 (non-ionic) is 0.24 mM from the plot (Fig. 4) of absorbance ( $A$ ) versus  $[\text{TX-100}]_T$  at  $\lambda_{\text{max}} = 460$  nm. The plot has a break in the region of CMC for solutions containing the mixture of TX-100 and  $I_2$  solution. It has similarity with the plots reported in earlier literature [31, 32]. The peak at 460 nm for iodine is continuously blue-shifted with increasing the concentration of TX-100 (Fig. 5).

### Product analysis

Substrate glycerol was taken 15 times higher than  $[\text{Cr(VI)}]_T$  and dissolved in  $0.5 \text{ mol dm}^{-3} \text{ H}_2\text{SO}_4$  making a total volume of the solution of  $200 \text{ cm}^3$ . The reaction mixture was heated and evaporated to a small volume to get a concentrated solution. It is important to mention that the substrate was taken at least 10 times higher than the oxidant maintaining pseudo-first-order criteria. The selectivity of the oxidation was maintained such that no further oxidation of the aldehyde would occur. Oxidation was made selective from glycerol to glyceraldehyde by stopping the over-oxidation of glyceraldehyde. The change in the color from yellow to pale greenish blue ensures the completion of the reaction. The appearance of the first

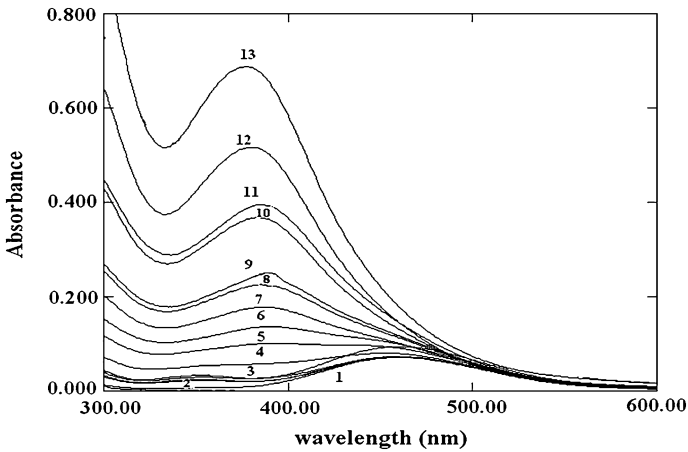


**Fig. 5** Absorption spectra of saturated aqueous solution of  $I_2$  in the absence and presence of TX-100 at 30 °C. Spectra-1 saturated  $I_2$  solution in the absence of TX-100; spectra 2–13,  $[TX-100]_T = 10 \times 10^{-5}$  (M),  $15 \times 10^{-5}$  (M),  $20 \times 10^{-5}$  (M),  $25 \times 10^{-5}$  (M),  $30 \times 10^{-5}$  (M),  $35 \times 10^{-5}$  (M),  $40 \times 10^{-5}$  (M),  $45 \times 10^{-5}$  (M),  $50 \times 10^{-5}$  (M),  $75 \times 10^{-5}$  (M),  $100 \times 10^{-5}$  (M), and  $125 \times 10^{-5}$  (M), respectively

prominent greenish blue color confirms the total conversion of Cr(VI) to Cr(III). After completion of the reaction, the product was isolated by fractional distillation. A small portion of the distilled product was treated with 2,4-dinitrophenyl hydrazine (DNP) in ethanolic  $H_2SO_4$  media. The mixture was allowed to settle down for half an hour. The yellowish orange-colored precipitate of the 2,4-dinitrophenyl hydrazone derivative was filtered off, dried in an oven, and recrystallized from ethanol. The same was also performed for the micelle-catalyzed reactions in the presence of promoters. The melting point of the recrystallized hydrazone substance was obtained at 169 °C which matches with the reported [27, 33–35] value of the glyceraldehyde-DNP derivative. The IR spectrum (Fig. 6) of the 2,4-DNP derivative of the product was recorded by the Perkin-Elmer FTIR model RX1 spectrometer. The IR spectrum of glyceraldehyde-DNP derivative observed is similar to the earlier literature work [33]. Melting point data and IR spectrum of hydrazone strongly support the identity of the product as glyceraldehyde from oxidation of glycerol.

## Materials

Glycerol (AR, SRL) was purified by refluxing with an excess of freshly burnt quicklime followed by distillation, and purity was checked by density measurement. 2,2'-bipyridine (AR, Qualigens), SDS (AR, SRL), CPC (AR, SRL), TX-100 (AR, SRL), 2,4-dinitrophenyl hydrazine (DNP) (AR, Qualigens), and Iodine (AR, Merck), and all other necessary chemicals used were of highest purity available commercially. Solutions were prepared by using double-distilled water.

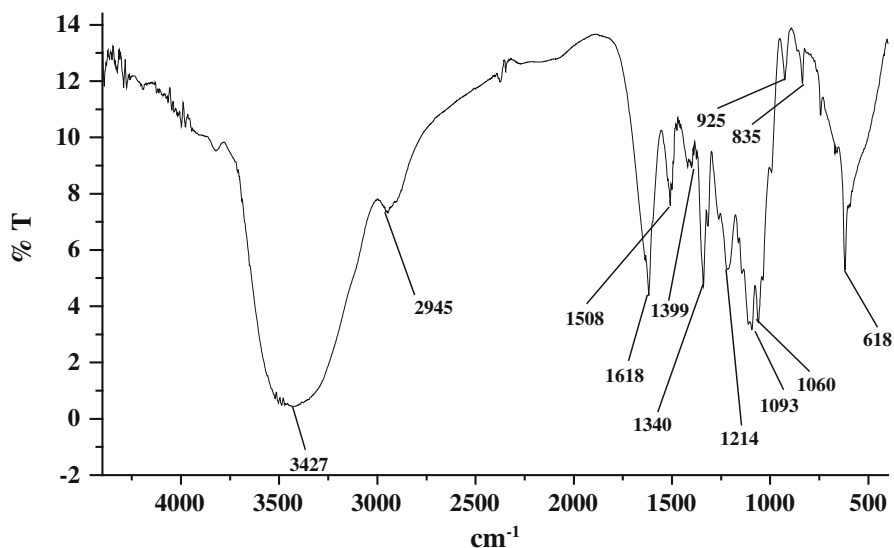


**Fig. 6** IR spectrum of 2,4-dinitrophenylhydrazone of glyceraldehyde

## Results and discussion

### Dependence on Cr(VI)

Under the kinetic and experimental conditions  $[\text{glycerol}]_{\text{T}} \gg [\text{Cr(VI)}]_{\text{T}}$  both in the presence and absence of bipy, the rate of disappearance of Cr(VI) showed a first-order dependence on  $[\text{Cr(VI)}]_{\text{T}}$ . The first-order dependence on Cr(VI) was also maintained in the presence of the three non-functional surfactants, CPC, SDS and TX-100. The pseudo-first-order rate constants  $k_{\text{obs}}$  were directly evaluated from the slope of the linear plot of  $\log [\text{Cr(VI)}]_{\text{T}}$  versus time ( $t$ ) [27, 36].

### Dependence on substrate

From previous work, it has been observed that the rate of the reaction was first-order with respect to substrate [27, 36], and this was also true in the presence of surfactants.

### Dependence on $\text{H}^+$

The reaction is second-order with respect to  $\text{H}^+$  ion concentration which has been previously observed [27].

### Dependence on $[\text{bipy}]_{\text{T}}$

The plots of  $k_{\text{obs(T)}}$  versus  $[\text{bipy}]_{\text{T}}$  are linear with positive intercepts measuring the contribution of rate enhancement over the unpromoted path (Fig. 7). The pseudo-first-

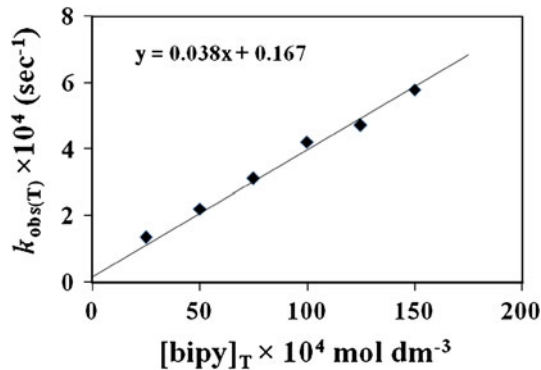


**Fig. 7** Dependence of  $k_{\text{obs}(T)}$  on  $[\text{bipy}]_T$  for Cr(VI) oxidation of glycerol (in the absence of surfactant) in aqueous  $\text{H}_2\text{SO}_4$  media at  $30^\circ\text{C}$ .  $[\text{Cr(VI)}]_T = 5 \times 10^{-4} \text{ mol dm}^{-3}$ ,  $[\text{glycerol}]_T = 75 \times 10^{-4} \text{ mol dm}^{-3}$ ,  $[\text{H}_2\text{SO}_4]_T = 0.5 \text{ mol dm}^{-3}$

order rate constant  $k_{\text{obs}(u)}$  calculated in the absence of bipy under the same conditions nicely matches with those obtained from the intercepts of plots of  $k_{\text{obs}(T)}$  versus  $[\text{bipy}]_T$  [27]. The observation can be formulated as:  $k_{\text{obs}(T)} = k_{\text{obs}(u)} + k_{\text{cat}}[\text{bipy}]_T$ .

Spectrophotometric analysis of the reaction

#### UV-Vis spectra

The gradual production of the Cr(III) species was confirmed spectrophotometrically. In the unpromoted path, the final color appeared as pale blue ( $\lambda_{\text{max}} = 583$  and  $260 \text{ nm}$ ; Fig. 8) which is quite different from the color observed in the bipy-

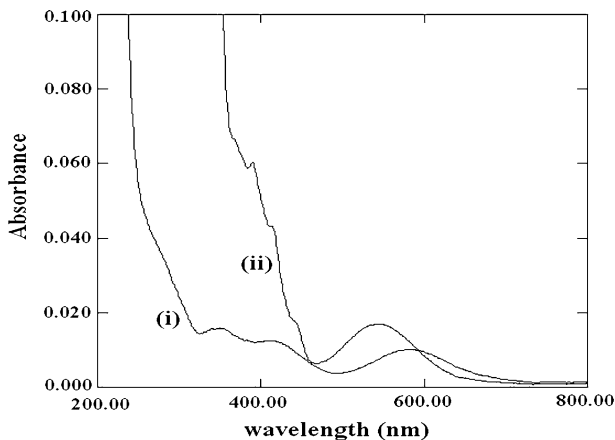


**Fig. 8** Absorption Spectrum of reaction mixture (after completion of reaction):  $[\text{glycerol}]_T = 75 \times 10^{-4} \text{ mol dm}^{-3}$ ,  $[\text{Cr(VI)}]_T = 5 \times 10^{-4} \text{ mol dm}^{-3}$ ,  $[\text{H}_2\text{SO}_4]_T = 0.5 \text{ mol dm}^{-3}$ , Temp =  $30^\circ\text{C}$  (i) unpromoted: (The spectrum of the chromic sulfate is identical with this under the experimental condition), (ii) bipy promoted:  $[\text{bipy}]_T = 0.01 \text{ mol dm}^{-3}$

promoted path which was pale violet ( $\lambda_{\max} = 544$  nm, Fig. 8). In the unpromoted path, two peaks were found due to the transitions [37, 38]  $\lambda_{\max} = 583$  nm for  ${}^4A_{2g}(F) \rightarrow {}^4T_{2g}(F)$  and  $\lambda_{\max} = 260$  nm for  ${}^4A_{2g}(F) \rightarrow {}^4T_{1g}(F)$  of Cr(III), respectively. The spectra of the final solution in the absence of promoter and pure chromic sulphate solution in aqueous sulphuric acid media are almost similar, but different due to the presence of different types of Cr(III)-species ( $\lambda_{\max} = 544$  nm for the bipy-promoted path; Fig. 8). This simply suggests that the final Cr(III)-aqua species are the Cr(III)-bipy complex. Similar results were reported by earlier workers [39]. In the bipy-promoted reaction path, there is a hypsochromic (blue) shift for the transition  ${}^4A_{2g}(F) \rightarrow {}^4T_{2g}(F)$  compared to the final solution of the unpromoted reaction path (Fig. 7a). The blue shift for the transition  ${}^4A_{2g}(F) \rightarrow {}^4T_{2g}(F)$  in the Cr(III)-bipy complex is due to the presence of the strong field bipy ligand compared to the aqueous ligand. For the Cr(III)-bipy complex [23, 39], the band due to the transition  ${}^4A_{2g}(F) \rightarrow {}^4T_{1g}(F)$  merges with a charge-transfer band (Fig. 8). Here, the appearance of the charge-transfer at much lower energy (visible range) for the proposed Cr(III)-bipy complex is significant due to the favored metal to ligand charge-transfer. The vacant  $\pi^*$  (antibonding) M.O. of the ligand (bipy) switches the metal to ligand electron-transfer (MLCT). These facts are supported by previous work [38–40]. The presence of the charge-transfer band (MLCT) at this lower energy (higher wave length) for the bipy-promoted reaction supports the formation of the Cr(III)-bipy complex in the final solution.

The reaction solutions were scanned in the range 400–700 nm in both the presence and absence of promoter and surfactant at regular time intervals (3–4 min) to follow the gradual development of the reaction intermediates (if any) and the product. The scanned spectra (Fig. 9a) indicate the gradual disappearance of Cr(VI) species and the appearance of Cr(III) species with an isobestic point at  $\lambda_{\max} = 533$  nm for the unpromoted reaction. In the presence of only the promoter (bipy), the isobestic points appeared at  $\lambda_{\max} = 519$  nm (Fig. 9b). In the presence of SDS and bipy, the scanned spectrum could not be recorded as the reaction was too fast to monitor. The isobestic point of the TX-100 catalyzed bipy-promoted reaction path was found at  $\lambda_{\max} = 512$  nm (Fig. 9c). It is interesting to note that, under the present experimental and kinetic conditions, the appearance of the single isobestic point in each scanned spectra firmly suggests the formation of very low concentrations or short-lived intermediates like Cr(V) and Cr(IV) [41] during the oxidation. In such cases, because of the very low concentration of the species, it may not always be possible to detect the species spectrophotometrically [42]. In the bipy-promoted reaction path, the active oxidant involved in the oxidation process is Cr(VI)-bipy (Fig. 10) [5, 23, 26–28].

### Mechanism of the reaction and rate law

Product analysis and spectroscopic results indicate that glyceraldehyde was the major oxidized product, i.e. oxidation of the single primary hydroxyl group occurred. The mechanism of the reaction can be divided into two parts: (1) the unpromoted path and (2) the promoted path. The unpromoted path for chromic acid oxidation of glycerol (Scheme 1) has been established earlier [27].

**Fig. 9 a** Scanned absorption spectra of the reaction mixture in absence of promoter at regular time intervals (5 min).  $[\text{glycerol}]_T = 75 \times 10^{-4} \text{ mol dm}^{-3}$ ,  $[\text{Cr(VI)}]_T = 5 \times 10^{-4} \text{ mol dm}^{-3}$ ,  $[\text{H}_2\text{SO}_4]_T = 0.5 \text{ mol dm}^{-3}$ .  $\lambda_{\text{isobestic}} = 533 \text{ nm}$ . Temp =  $30^\circ\text{C}$ . **b** Scanned absorption spectra of the reaction mixture at regular time intervals (3 min).  $[\text{glycerol}]_T = 75 \times 10^{-4} \text{ mol dm}^{-3}$ ,  $[\text{Cr(VI)}]_T = 5 \times 10^{-4} \text{ mol dm}^{-3}$ ,  $[\text{H}_2\text{SO}_4]_T = 0.5 \text{ mol dm}^{-3}$ ,  $[\text{bipy}]_T = 125 \times 10^{-4} \text{ mol dm}^{-3}$ .  $\lambda_{\text{isobestic}} = 519 \text{ nm}$ . Temp =  $30^\circ\text{C}$ . **c** Scanned absorption spectra of the reaction mixture at regular time intervals (3 min).  $[\text{glycerol}]_T = 75 \times 10^{-4} \text{ mol dm}^{-3}$ ,  $[\text{Cr(VI)}]_T = 5 \times 10^{-4} \text{ mol dm}^{-3}$ ,  $[\text{H}_2\text{SO}_4]_T = 0.5 \text{ mol dm}^{-3}$ ,  $[\text{bipy}]_T = 75 \times 10^{-4} \text{ mol dm}^{-3}$ ,  $[\text{TX-100}]_T = 2 \times 10^{-2} \text{ mol dm}^{-3}$ .  $\lambda_{\text{isobestic}} = 512 \text{ nm}$ . Temp =  $30^\circ\text{C}$

In this path, attachment of  $\text{H}^+$  with the neutral ester (**1**) formed during the process facilitates the decomposition of the protonated ester (**2**) and gives rise to the product glyceraldehyde [27]. In the unpromoted path, the rate law is:  $k_{\text{obs}} = (2/3) k_1 K_1 K_2 [\text{glycerol}]_T [\text{H}^+]^2$ . In the bipy-promoted reaction path, the formation of the Cr(III)-bipy complex characterized spectrophotometrically indicates that the promoter (bipy) used here undergoes complexation with the highest oxidation states of chromium (labile,  $t_{2g}^0 e_g^0$ ). Based on this concept, it is believed that the Cr(VI)-bipy complex (complex  $C_1$ ) produced in the pre-equilibrium step is the active oxidant (mentioned as  $\text{AO}^+$  in Scheme 2). This complex species reacts with the substrate glycerol to produce a ternary complex  $C_2$ , and it would undergo redox decomposition via several steps to produce the Cr(III)-bipy complex. The mechanism of the bipy-promoted reaction path can be established as follows

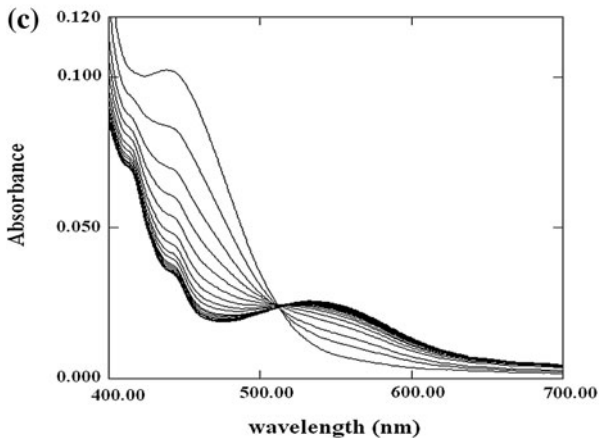
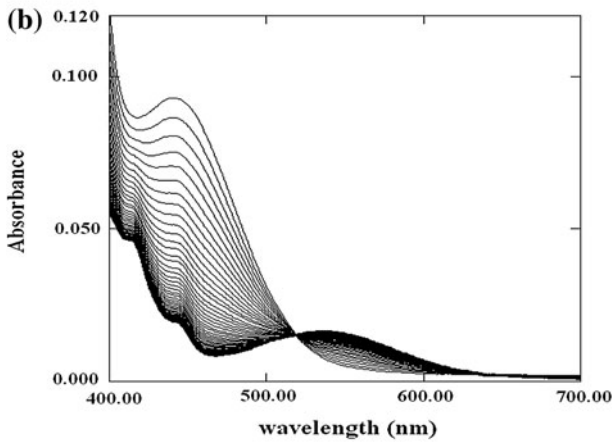
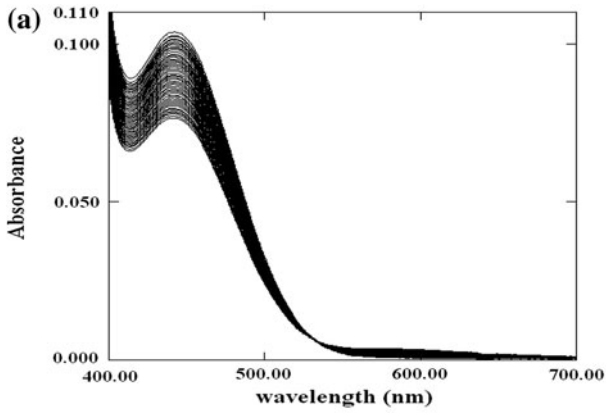
Derivation of rate law (considering Scheme 2):

$$\begin{aligned}
 K_3 &= \frac{[C_1]}{[\text{bipyH}^+][\text{H}^+]^2[\text{HCrO}_4^-]} \\
 K_4 &= \frac{[C_2][\text{H}_3\text{O}^+]}{[\text{glycerol}][C_1]} \\
 \text{rate} &= \frac{d[\text{glycerol}]}{dt} = -\frac{d\ln[\text{HCrO}_4^-]}{dt} = k_3[C_2] \\
 &= \frac{k_3 K_4 [\text{glycerol}][C_1]}{[\text{H}_3\text{O}^+]} \\
 &= \frac{k_3 K_3 K_4 [\text{glycerol}][\text{bipyH}^+][\text{H}^+]^2[\text{HCrO}_4^-]}{[\text{H}_3\text{O}^+]}
 \end{aligned}$$

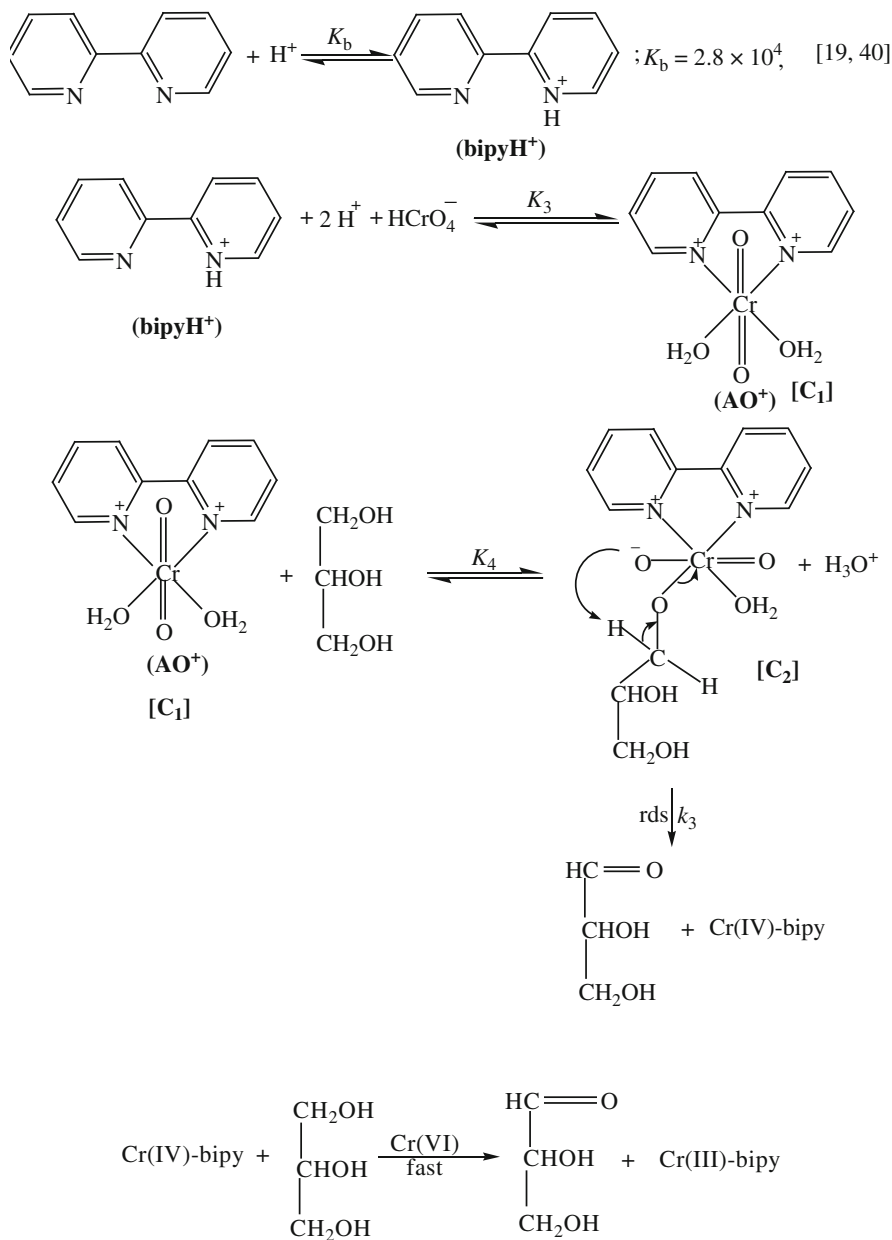
The total concentration of bipy is given by:

$$\begin{aligned}
 [\text{bipyH}^+]_T &= [\text{bipy}] + [\text{bipyH}^+] \\
 K_b &= \frac{[\text{bipyH}^+]}{[\text{bipy}][\text{H}^+]}; \text{ or } [\text{bipy}] = \frac{[\text{bipyH}^+]}{K_b[\text{H}^+]} \\
 \text{or } [\text{bipy}]_T &= \frac{[\text{bipyH}^+]}{K_b[\text{H}^+]} + [\text{bipyH}^+] = [\text{bipyH}^+] \times \left[ 1 + \frac{1}{K_b[\text{H}^+]} \right] \\
 &= [\text{bipyH}^+] \times \left[ \frac{K_b[\text{H}^+] + 1}{K_b[\text{H}^+]} \right] \approx [\text{bipyH}^+]
 \end{aligned}$$

Since,  $K_b[\text{H}^+] \gg 1$ ,  $K_b = 2.8 \times 10^4$  for bipy






**Scheme 2** Cr(VI) oxidation of glycerol in presence of bipy

$$\begin{aligned} \text{rate} &= -\frac{d[\text{HCrO}_4^-]}{dt} = \frac{k_3 K_3 K_4 [\text{glycerol}] [\text{bipyH}^+] [\text{H}^+]^2 [\text{HCrO}_4^-]}{[\text{H}_3\text{O}^+]} \\ &= k_3 K_3 K_4 [\text{glycerol}] [\text{bipy}] [\text{HCrO}_4^-] [\text{H}^+] \end{aligned}$$

and

$$\begin{aligned} -\frac{1}{2} \frac{d[\text{HCrO}_4^-]}{dt} &= \frac{1}{3} \frac{d[\text{glycerol}]}{dt} \\ -\frac{d \ln [\text{HCrO}_4^-]}{dt} &= k_{\text{obs(c)}} = \frac{2}{3} k_3 K_3 K_4 [\text{glycerol}] [\text{bipy}] [\text{H}^+] \end{aligned}$$

The rate law of bipy-promoted reaction path can be proposed as:

$$k_{\text{obs(c)}} = (2/3) k_3 K_3 K_4 [\text{glycerol}] [\text{bipy}] [\text{H}^+]$$

### Effect of the non-functional micellar catalysts on the reaction rate

The surfactant comprises a hydrophilic and a hydrophobic group. The different interaction of these two moieties with water is an important cause for surfactants to aggregate into micelles and other nanometer-scale structures in aqueous solution [43].

### Partitioning of reactant in unpromoted path

In the unpromoted reaction path, partitioning of the neutral ester [(1) Scheme 1] in all types of the surfactants is almost equally probable (Fig. 11). The phenomenon of partitioning of proton in the unpromoted reaction path is highest for the anionic surfactant SDS due to favorable and very effective electrostatic attraction. Thus, for SDS, the reaction goes on in both aqueous and micellar phases where the active reactants are preferably accumulated [42]. Thus, SDS allows the reaction to proceed in both aqueous and micellar interphases [44]. TX-100, a neutral surfactant, retards the rate of oxidation process slightly lower than pure water, as there are no charge head groups present [28]. Again, with gradual increasing of the concentration of TX-100, the rate of oxidation is decreased. These data are not shown in the text. The decrease in electrostatic attraction between the approaching  $\text{H}^+$  ion and the large hydrophobic group of neutral TX-100 is significant for the observed rate retardation. The rate of oxidation of glycerol is first-order with respect to substrate, i.e. glycerol as observed from previous literature [27]. A severe electrostatic repulsion between the approaching  $\text{H}^+$  ion and the positive hydrophilic head group of cationic CPC makes unavailable the effective concentration of neutral ester and  $\text{H}^+$  within the micellar core. Consequently, the reaction is restricted only in aqueous phase where the concentration of the ester species is depleted due to its preferential partitioning in the micellar pseudo-phase. Thus, CPC shows the rate-retarding effect even from pure water [42].

### Partitioning of reactant in the promoted path

The most pronounced acceleration of the oxidation process is observed in the SDS-catalyzed bipy-promoted path (Table 3). In this path, the Cr(VI)–bipy complex,

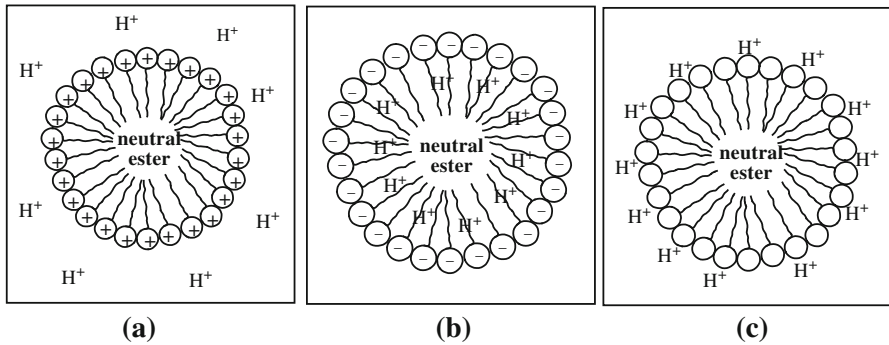


**Fig. 11** Schematic representation of partitioning of neutral ester and proton in **a** cationic surfactant, **b** anionic surfactant, and **c** neutral surfactant

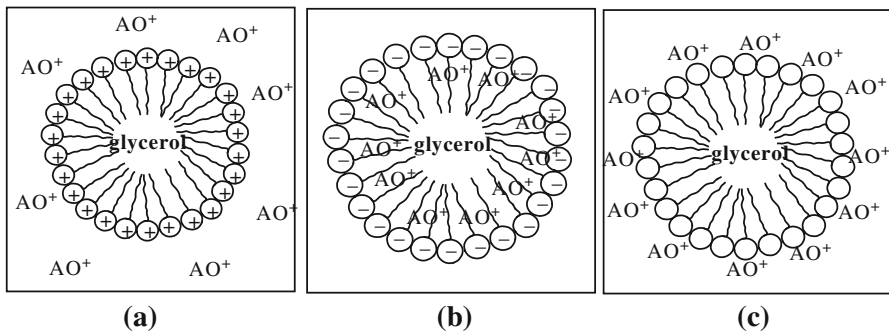


**Fig. 12** Schematic representation of the partitioning of substrate and active oxidant [AO<sup>+</sup> = Cr(VI)-promoter complex] in **a** cationic surfactant, **b** anionic surfactant, and **c** neutral surfactant

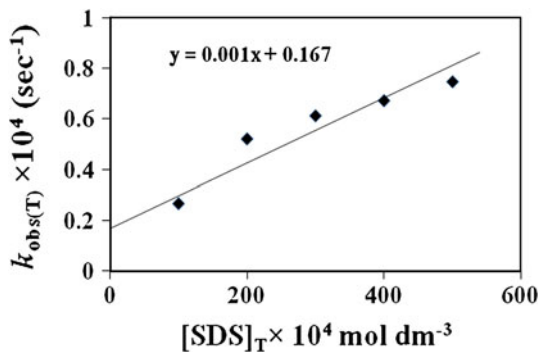


**Fig. 13** Dependence of  $[\text{SDS}]_{\text{T}}$  on  $k_{\text{obs(T)}}$  for Cr(VI) oxidation of glycerol in the absence of the promoter in aqueous  $\text{H}_2\text{SO}_4$  media at 30 °C.  $[\text{Cr(VI)}]_{\text{T}} = 5 \times 10^{-4} \text{ mol dm}^{-3}$ ,  $[\text{glycerol}]_{\text{T}} = 75 \times 10^{-4} \text{ mol dm}^{-3}$ ,  $[\text{H}_2\text{SO}_4]_{\text{T}} = 0.5 \text{ mol dm}^{-3}$

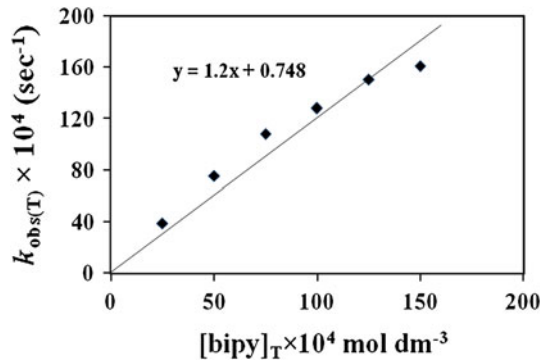


**Fig. 14** Dependence of  $k_{\text{obs}(T)}$  on  $[\text{bipy}]_T$  for the Cr(VI) oxidation of glycerol in the presence of the surfactant  $[\text{SDS}]_T$  in aqueous  $\text{H}_2\text{SO}_4$  media at 30 °C.  $[\text{Cr(VI)}]_T = 5 \times 10^{-4} \text{ mol dm}^{-3}$ ,  $[\text{glycerol}]_T = 75 \times 10^{-4} \text{ mol dm}^{-3}$ ,  $[\text{H}_2\text{SO}_4]_T = 0.5 \text{ mol dm}^{-3}$ ,  $[\text{SDS}]_T = 5 \times 10^{-2} \text{ mol dm}^{-3}$

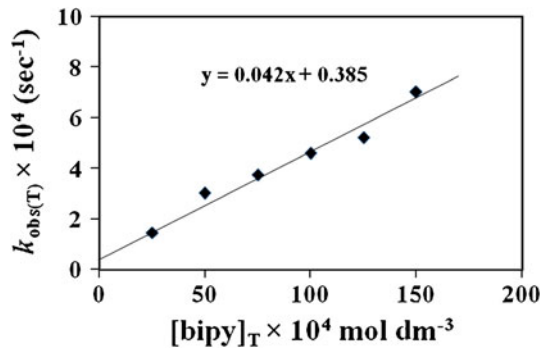


**Fig. 15** Dependence of  $k_{\text{obs}(T)}$  on  $[\text{promoter}]_T$  for the Cr(VI) oxidation of glycerol in the presence of the surfactant  $[\text{TX-100}]_T$  in aqueous  $\text{H}_2\text{SO}_4$  media at 30 °C.  $[\text{Cr(VI)}]_T = 5 \times 10^{-4} \text{ mol dm}^{-3}$ ,  $[\text{glycerol}]_T = 75 \times 10^{-4} \text{ mol dm}^{-3}$ ,  $[\text{H}_2\text{SO}_4]_T = 0.5 \text{ mol dm}^{-3}$ ,  $[\text{TX-100}]_T = 2 \times 10^{-2} \text{ mol dm}^{-3}$

represented as  $\text{AO}^+$  (Fig. 12, Scheme 2), a cationic complex, has been argued as the active oxidant. Because of the electrostatic attraction, it can preferably be distributed in the micellar pseudo-phase of the anionic surfactant SDS. Thus, in the presence of SDS, the reaction can propagate in both the micellar pseudo-phase (where both the active oxidant and substrate are preferably concentrated) and the aqueous phase to give the observed rate acceleration [27, 42]. The plots of  $k_{\text{obs}(T)}$  versus  $[\text{SDS}]_T$  (Fig. 13) and  $k_{\text{obs}(T)}$  versus  $[\text{bipy}]_T$  (Fig. 14) exhibit a continuous increase up to the concentration of SDS (for the unpromoted path) and bipy used for the SDS-catalyzed bipy-promoted reaction path. A similar effect is observed for the combination of TX-100 micelles and bipy, but the increase of the oxidation rate (Fig. 15) is smaller because the degree of glycerol binding to the nonionic surfactant micelles is probably smaller compared with the degree of binding to the anionic ones [45]. The active oxidant Cr(VI)–bipy complex reacts with glycerol to form a ternary complex which undergoes redox decomposition in a rate-limiting step [46, 47], giving rise to the product. In the case of TX-100, Cr(VI)–bipy also approaches

**Table 2**  $k_{\text{obs}}$  and half life of the reaction in presence and absence of bipy and non-functional micellar catalyst

Promoter (mol dm <sup>-3</sup> )	Micellar catalyst (mol dm <sup>-3</sup> )	$10^4 \times k_{\text{obs}}$ (s <sup>-1</sup> )	$t_{1/2}$ (h)
None	None	$0.167 \pm 0.03$	11.54
2,2'-bipyridine (bipy)	None		
0.0025		$1.358 \pm 0.03$	1.41
0.005		$2.211 \pm 0.04$	0.87
0.075		$3.121 \pm 0.02$	0.616
0.01		$4.218 \pm 0.02$	0.45
0.0125		$4.713 \pm 0.03$	0.40
0.015		$5.793 \pm 0.04$	0.33
None	CPC		
	0.002	$0.0065 \pm 0.02$	29.61
None	SDS		
	0.01	$0.267 \pm 0.04$	7.2
	0.02	$0.5216 \pm 0.04$	3.69
	0.03	$0.6133 \pm 0.05$	3.14
	0.04	$0.6733 \pm 0.06$	2.86
	0.05	$0.7483 \pm 0.03$	2.57
None	TX-100		
	0.02	$0.3833 \pm 0.03$	15.83
2,2'-bipyridine (bipy)	SDS		
0.0025	0.05	$38.9 \pm 0.04$	0.049
0.005		$75.3 \pm 0.06$	0.0255
0.075		$108.2 \pm 0.05$	0.0177
0.01		$128 \pm 0.03$	0.015
0.0125		$150.6 \pm 0.02$	0.0127
0.015		$161.1 \pm 0.04$	0.0116
2,2'-bipyridine (bipy)	TX-100		
0.0025	0.02	$1.46 \pm 0.03$	1.318
0.005		$3.017 \pm 0.04$	0.638
0.075		$3.738 \pm 0.02$	0.515
0.01		$4.585 \pm 0.05$	0.42
0.0125		$5.213 \pm 0.04$	0.37
0.015		$7.015 \pm 0.03$	0.274

$[\text{Cr(VI)}]_{\text{T}} = 5 \times 10^{-4} \text{ mol dm}^{-3}$ ,  $[\text{H}_2\text{SO}_4] = 0.5 \text{ mol dm}^{-3}$ ,  $[\text{glycerol}]_{\text{T}} = 75 \times 10^{-4} \text{ mol dm}^{-3}$ , Temp = 30 °C

to the neutral head group of the micelle, but the amount is less compared to SDS because TX-100 is a neutral surfactant, so no electrostatic attraction takes place [28, 48]. The degree of rate enhancement in the TX-100-catalyzed bipy-promoted path is most probably due to the continuous increase of Cr(VI)–bipy complexes upon

**Table 3** Kinetic parameters and some representative  $k_{\text{eff}}$  values for the Cr(VI) oxidation of glycerol in the presence of bipyand catalyst (surfactant) in aqueous  $\text{H}_2\text{SO}_4$  media

Promoter	Micellar catalyst	$k_{\text{eff}}(\text{bipy})(w)$	$k_{\text{eff}}(s)(w)$	$k_{\text{eff}}(\text{bipy})(s)$
2,2'-bipyridine (bipy)	None	33.68	–	–
None	SDS	–	3.48	–
2,2'-bipyridine (bipy)	SDS	–	–	214.37
2,2'-bipyridine (bipy)	TX-100	–	–	17.316

$W$  = water,  $S$  = surfactant,  $[\text{Cr(VI)}]_{\text{T}} = 5 \times 10^{-4} \text{ mol dm}^{-3}$ ,  $[\text{H}_2\text{SO}_4] = 0.5 \text{ mol dm}^{-3}$ ,  $[\text{glycerol}]_{\text{T}} = 75 \times 10^{-4} \text{ mol dm}^{-3}$ ,  $[\text{Promoter}]_{\text{T}} = 150 \times 10^{-4} \text{ mol dm}^{-3}$ ,  $[\text{SDS}]_{\text{T}} = 5 \times 10^{-2} \text{ mol dm}^{-3}$ ,  $[\text{TX-100}]_{\text{T}} = 2 \times 10^{-2} \text{ mol dm}^{-3}$ , Temp = 30 °C

increasing the concentration of bipy, forcefully allowing the reaction with glycerol within the large hydrophobic core. In this study, the combination of CPC and bipy are not used due to the rate retardation effect of CPC in the absence of the promoter.

From Table 2, it is confirmed that the rate is continuously increasing with the increase in the concentration of bipy in the presence and absence of micelles (Fig. 7). Rate enhancement is small for TX-100 compared to SDS, but CPC retards the oxidation process as is evident from the  $t_{1/2}$  value in Table 2. Rate acceleration is highest when SDS and bipy are combined (Fig. 14). The total time taken to complete the oxidation process gradually shortens with increasing the concentration of bipy for a fixed concentration of SDS. Plots of  $k_{\text{obs(T)}}$  versus  $[\text{bipy}]_{\text{T}}$  and  $[\text{SDS}]_{\text{T}}$  are linear with positive intercepts (Figs. 12, 13, 14, 15). In each micelle–bipy combined set of experiments, the values of  $k_{\text{obs(T)}}$  are increased in a regular fashion upon further increasing the bipy concentration at the fixed surfactant concentration. The pseudo-first-order rate constants ( $k_{\text{obs}}$ ,  $\text{s}^{-1}$ ) were determined from the slope of plots of  $\ln(A_{450})$  against time ( $t$ ) at wave length 450 nm. The  $t_{1/2}$  values are directly calculated in Table 2 by using the relationship  $t_{1/2} = (\ln 2/k_{\text{obs}})$ , where  $k_{\text{obs}}$  = pseudo-first-order rate constant.

Another kinetic parameter has been introduced in Table 3 which can be defined as the efficiency of only the promoter or only the catalyst or both (combination of promoter and catalyst) to catalyze, promote, and accelerate the reaction process, and is termed  $k_{\text{eff}}$ . The  $k_{\text{eff}}$  values are directly calculated from the relationship  $k_{\text{eff}} = \{k_{\text{obs(T)}} - k_{\text{obs(u)}}\}/k_{\text{obs(u)}}$  under the kinetic and experimental conditions, where  $k_{\text{obs(T)}}$  = rate constant of the promoted path and  $k_{\text{obs(u)}}$  = rate constant of the unpromoted path. The plot of  $k_{\text{obs(T)}}$  versus  $[\text{SDS}]_{\text{T}}$  (Fig. 13) shows a continuous increase up to the concentration of SDS used for the unpromoted path. From Table 3 (Fig. 14), the value of  $k_{\text{eff}} = 214.37$  at the highest concentration of SDS and bipy strongly suggests that this combination is the most effective one among all the micelle–bipy combinations. The combination of SDS and bipy in the reaction mixture leads to almost kilo-fold (994 times faster) acceleration compared to the uncatalyzed and unpromoted path. From the plot of  $k_{\text{obs(T)}}$  versus bipy (Fig. 7), it is clear that  $k_{\text{obs}}$  is almost proportional to the concentration of bipy added in the reaction mixture. The value of  $k_{\text{obs}}$  has been increased linearly with increasing the concentration of SDS (Fig. 13). The surfactant SDS also has an effect on the bipy-promoted reaction path, and rate constants are found to be increased (Fig. 14) upon

**Table 4** A comparative result for oxidation of glycerol using different oxidant and catalyst

Entry	Promoter	Catalyst	Reference	Conditions	Reaction rate sec <sup>-1</sup>
1	Picolinic acid = 0.01 mol dm <sup>-3</sup>	-	[27]	[glycerol] = 0.01 mol dm <sup>-3</sup> , [Cr(VI)] = 0.0005 mol dm <sup>-3</sup> , [H <sup>+</sup> ] = 0.50 mol dm <sup>-3</sup> , T = 30°C	7.022 × 10 <sup>-5</sup>
2	Picolinic acid = 0.01 mol dm <sup>-3</sup>	SDS = 0.02 mol dm <sup>-3</sup>	[27]	[glycerol] = 0.01 mol dm <sup>-3</sup> , [Cr(VI)] = 0.0005 mol dm <sup>-3</sup> , [H <sup>+</sup> ] = 0.50 mol dm <sup>-3</sup> , T = 30°C	1.513 × 10 <sup>-4</sup>
3	-	Ru(III) = 9.60 × 10 <sup>-6</sup> mol dm <sup>-3</sup>	[49]	[glycerol] = 2.0 × 10 <sup>-2</sup> mol dm <sup>-3</sup> , [KBrO <sub>3</sub> ] = 33.33 × 10 <sup>-4</sup> mol dm <sup>-3</sup> , [Hg(OAc) <sub>2</sub> ] = 1 × 10 <sup>-3</sup> mol dm <sup>-3</sup> , [H <sup>+</sup> ] = 0.01 mol dm <sup>-3</sup> , [KCl] = 10 × 10 <sup>-4</sup> mol dm <sup>-3</sup> , [NaClO <sub>4</sub> ] = 1.1 × 10 <sup>-2</sup> mol dm <sup>-3</sup> , 45°C	7.64 × 10 <sup>-4</sup>
4	2,2'-bipyridine = 0.015 mol dm <sup>-3</sup>	-	Present work	[glycerol] = 75.0 × 10 <sup>-4</sup> mol dm <sup>-3</sup> , [Cr(VI)] = 0.0005 mol dm <sup>-3</sup> , [H <sup>+</sup> ] = 0.50 mol dm <sup>-3</sup> , T = 30°C	5.793 × 10 <sup>-4</sup>
5	2,2'-bipyridine = 0.015 mol dm <sup>-3</sup>	SDS = 0.05 mol dm <sup>-3</sup>	Present work	[glycerol] = 75.0 × 10 <sup>-4</sup> mol dm <sup>-3</sup> , [Cr(VI)] = 0.0005 mol dm <sup>-3</sup> , [H <sup>+</sup> ] = 0.50 mol dm <sup>-3</sup> , T = 30°C	161.1 × 10 <sup>-4</sup>

increasing the concentration of bipy at a fixed SDS concentration. A similar type of dependence pattern has also been observed in the presence of TX-100 on the promoted reaction path with enhanced rate constants (Fig. 15).

The slope obtained from the plot of the combination of SDS and bipy path is very steep compared with the TX-100–bipy combination path.

A comparison table (Table 4) explains the selection of suitable catalysts and promoters over the other oxidants used previously in glycerol to glyceraldehydes conversion:

## Conclusion

The main target of this study was to carry out the oxidation in aqueous micellar media at room temperature. In this context, the use of water as solvent features many benefits, not only because water itself is innocuous but because it can also potentially improve reactivities and selectivities, simplify the workup procedures, enable the recycling of the micellar catalyst, and allowing mild reaction conditions and protecting group-free synthesis. Oxidation is made selective to glyceraldehyde by stopping the over-oxidation of glyceraldehyde by maintaining pseudo-first-order conditions. The remaining glycerol can be re-oxidized to the deserved product with the addition of chromic acid maintaining the reaction condition the same. The CMC values of the three surfactants used are very helpful in determining the particular concentration of the surfactant to be used for the title reaction. The micelles act as nano-reactors and efficiently increase the effective concentration of the reactants into the small core inside it. It is interesting to note that the rate of oxidation is increased drastically when SDS is used as the micellar catalyst in combination with the bipy promoter at a particular concentration, whereas the cationic surfactant CPC and the neutral surfactant TX-100 inhibit the rate of oxidation. The Cr(VI)–bipy complex, a cationic species, has been found to act as the active oxidant in the bipy-promoted chromic acid oxidation of glycerol. The generation of Cr(III)-species after the completion of the oxidation of glycerol has been investigated by a series of spectra observed by UV–Vis spectrophotometry. The product aldehyde has also been confirmed by the conventional 2,4-DNP test and FTIR spectral analysis of the hydrazone derivative. The effects of the cationic, anionic, and neutral surfactants have been followed and the observed micellar effects are in agreement with the proposed reaction mechanism. These micellar effects are quite important to understand and to substantiate the proposed mechanistic pathways. The mechanistic paths of uncatalyzed unpromoted and SDS-catalyzed bipy-promoted chromic acid oxidation of glycerol have been compared. In conclusion, it can be said that anionic micelle SDS is an efficient micellar catalyst for the bipy-promoted chromic acid oxidation of glycerol to glyceraldehyde.

**Acknowledgments** Thanks to UGC, New Delhi and CSIR, New Delhi for providing financial help in the form of project and fellowship.

## References

1. B. Upasana, M.K. Chaudhuri, D. Dey, D. Kalita, W. Kharmawphlang, G.C. Mandal, *Tetrahedron* **57**, 2445 (2001)
2. S. Sundaram, P.S. Raghavan, *Chromium-VI Reagents: Synthetic Applications* (Springer, Heidelberg, 2011), 47
3. N. Feizi, H. Hassani, M. Hakimi, *Bull. Korean Chem. Soc.* **26**, 2084 (2005)
4. A.K. Das, S.K. Mondal, G. Mukherjee, *React. Kinet. Catal. Lett.* **73**, 257 (2001)
5. R. Saha, S.K. Ghosh, A. Ghosh, I. Saha, K. Mukherjee, A. Basu, B. Saha, *Res. Chem. Intermed.* **39**, 631 (2013)
6. A.L. Holmes, S.S. Wise, J.P. Wise, *Indian J. Med. Res.* **128**, 353 (2008)
7. R. Saha, R. Nandi, B. Saha, *J. Coord. Chem.* **64**, 1782 (2011)
8. B. Saha, C. Orvig, *Coord. Chem. Rev.* **254**, 2959 (2010)
9. A. Sivaprakash, R. Aravindhan, J.R. Rao, B.U. Nair, *Appl. Ecol. Env. Res.* **7**, 45 (2009)
10. A.K. Das, *Coord. Chem. Rev.* **248**, 81 (2004)
11. N. Dimitratos, A. Villa, L. Prati, *Catal. Lett.* **133**, 334 (2009)
12. A.V. Bryksin, P.P. Laktionov, *Biochemistry* **73**, 619 (2008)
13. N. Richter, M. Neumann, A. Liese, R. Wohlgemuth, A. Weckbecker, T. Eggert, W. Hummel, *Biotechnol. Bioeng.* **106**, 541 (2010)
14. P.K. Khatua, S. Ghosh, S.K. Ghosh, S.C. Bhattacharya, *J Disper Sci Technol* **25**, 741 (2004)
15. Z. Zhang, C.Y. Lin, *J. Photochem. Photobiol. A* **130**, 139 (2000)
16. M. Almgren, A. Valstar, *Langmuir* **15**, 2635 (1999)
17. M.A. Muherei, R. Junin, *J. Appl. Sci. Res.* **5**, 181 (2009)
18. S.K. Ghosh, R. Saha, K. Mukherjee, A. Ghosh, S.S. Bhattacharyya, B. Saha, *J. Korean Chem. Soc.* **56**, 164 (2012)
19. R. Saha, A. Ghosh, B. Saha, *Chem. Eng. Sci.* **99**, 23 (2013)
20. A. Ghosh, R. Saha, B. Saha, *J. Ind. Eng. Chem.* (2013). doi:10.1016/j.jiec.2013.03.028
21. A. Ghosh, R. Saha, K. Mukherjee, S.K. Ghosh, B. Saha, *Spectrochim. Acta A* **109**, 55 (2013)
22. K. Mukherjee, R. Saha, A. Ghosh, S.K. Ghosh, B. Saha, *Spectrochim. Acta A* **101**, 294 (2013)
23. J. Mandal, K.M. Chowdhury, K. Paul, B. Saha, *J. Coord. Chem.* **63**, 99 (2010)
24. R. Saha, A. Ghosh, P. Sar, I. Saha, S.K. Ghosh, K. Mukherjee, B. Saha, *Spectrochim. Acta Part A.* **116**, 524 (2013)
25. A. Ghosh, R. Saha, K. Mukherjee, S.K. Ghosh, S.S. Bhattacharyya, S. Laskar, B. Saha, *Int. J. Chem. Kinet.* **45**, 175 (2013)
26. R. Saha, A. Ghosh, B. Saha, *J. Coord. Chem.* **64**, 3729 (2011)
27. S.K. Ghosh, A. Basu, R. Saha, A. Ghosh, K. Mukherjee, B. Saha, *J. Coord. Chem.* **65**, 1158 (2012)
28. A. Ghosh, R. Saha, K. Mukherjee, S.K. Ghosh, S.S. Bhattacharyya, B. Saha, *J. Chem. Res.* **36**, 347 (2012)
29. A.A. Rafati, H. Gharibi, H. Houkhani, *Phys. Chem. Liq.* **39**, 521 (2001)
30. A. Domínguez, A. Fernández, N. González, E. Iglesias, L. Montenegro, *J. Chem. Educ.* **74**, 1227 (1997)
31. S.K. Hait, S.P. Moulik, *J. Surf. Deterg.* **4**, 303 (2001)
32. S. Ross, J.P. Oliver, *J. Phys. Chem.* **63**, 1671 (1959)
33. J.C. Underwood, H.G. Lento, J.C. Underwood, H.G. Lento, *Anal. Chem.* **32**, 1656 (1960)
34. A.I. Vogel, *Elementary Practical Organic Chemistry. Part III. Quantitative Organic Analysis*, 3rd edn. (ELBS and Longman Group Ltd., London, 1958), p. 739
35. F. Feigl, *Spot Tests in Organic Analysis*, vol. 342, 5th edn. (Elsevier, Amsterdam, 1956), p. 121
36. A. Basu, S.K. Ghosh, R. Saha, R. Nandi, T. Ghosh, B. Saha, *Tenside Surf. Deterg.* **48**, 453 (2011)
37. S.P. Meenakshisundaram, M. Gopalakrishnan, S. Nagarajan, N. Sarathi, *Catal. Commun.* **8**, 713 (2007)
38. B.N. Figgis, *Introduction to Ligand Fields* (Wiley Eastern Limited, New Delhi, 1966), p. 222
39. Z. Khan, K. Ud-Din, *Transition Met. Chem.* **27**, 832 (2002)
40. M. Islam, B. Saha, A.K. Das, *J. Mol. Catal. A* **266**, 21 (2007)
41. C.K. Jorgensen, *Absorption Spectra and Chemical Bonding in Complexes* (Pergamon, London, 1964), p. 290
42. B. Saha, M. Das, R.K. Mohanty, A.K. Das, *J. Chin. Chem. Soc.* **51**, 399 (2004)

43. K.S. Sharma, S.R. Patil, A.K. Rakshit, K. Glenn, M. Doiron, R.M. Palepu, P.A. Hassan, *J. Phys. Chem. B* **108**, 12804 (2004)
44. K. Mukherjee, R. Saha, A. Ghosh, S.K. Ghosh, B. Saha, *J. Mol. Liq.* **179**, 1 (2013)
45. S.J. Marta, M. Narkiewicz, *Colloid Polym. Sci.* **281**, 1142 (2003)
46. Z. Khan, S. Masan, Raju, K. Ud-Din, *Transition Met. Chem.* **28**, 881–887 (2003)
47. S. Meenakshisundaram, R. Markkandan, *Transition Met. Chem.* **29**, 308 (2004)
48. A. Basu, S.K. Ghosh, R. Saha, A. Ghosh, K. Mukherjee, B. Saha, *Tenside Surf. Deterg.* **50**, 249 (2013)
49. S. Shrivastava, H. Tripathi, K. Singh, *Transition Met. Chem.* **26**, 727 (2001)